

Topological quantum computing

Yaroslav Tserkovnyak

April 14, 2023

Contents

1	Topology of quantum statistics	2
1.1	Quantum statistics of elementary particles	2
1.2	(Classical) topology	3
1.3	The braid group	4
1.4	Quantum statistics of anyons	5
1.4.1	Fusion spaces	5
1.4.2	Fusion matrices	7
1.4.3	Braiding anyons	8
2	Quantum computing with anyons	10
2.1	Executing topological QC	10
2.2	Computing with Ising anyons	10
2.3	Majorana zero modes in superconducting wires	11
2.4	Universal computing with Fibonacci anyons	14

Chapter 1

Topology of quantum statistics

1.1 Quantum statistics of elementary particles

In basic quantum mechanics (or field theory), we construct multi-particle *Hilbert spaces* based on *tensor products* \otimes of single-particle spaces. For the latter, let us start with the simplest meaningful case of a two-dimensional space $\mathbb{S} = \{|0\rangle, |1\rangle\}$ spanned by some effective *spin up/down* states. This is the Hilbert space of a single *qbit*. A general physical state $|\psi\rangle$, which is normalized to unity, $\langle\psi|\psi\rangle = 1$, is represented (up to an overall phase) by two *Euler angles*, ϕ and θ , which place it on the *Bloch sphere*:

$$|\psi\rangle = \cos \frac{\theta}{2} |0\rangle + e^{i\phi} \sin \frac{\theta}{2} |1\rangle. \quad (1.1)$$

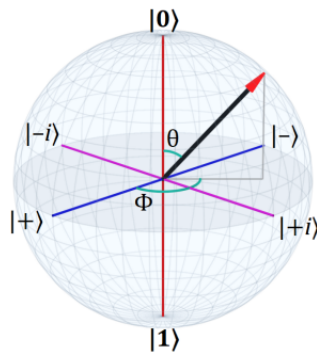


Figure 1.1: Bloch sphere representation of a qbit.

For two distinct qbits, the Hilbert space $\mathbb{G} = \mathbb{S}_1 \otimes \mathbb{S}_2$ is four-dimensional, spanned by $\{|00\rangle, |01\rangle, |10\rangle, |11\rangle\}$. If, however, two *indistinguishable* spin-1/2 particles, such as electrons, are strongly pinned in the same physical location (such as a *quantum dot*), their fundamental indistinguishability requires that their combined ket is an eigenstate of the *permutation operator* P :

$$P |\psi_1\rangle \otimes |\psi_2\rangle \equiv |\psi_2\rangle \otimes |\psi_1\rangle. \quad (1.2)$$

Since $P^2 = 1$, the only two possible eigenstates are $+1$ or -1 . The former corresponds to indistinguishable bosons, while the latter to fermions. Arranging \mathbb{G} according to the eigenvalues of $P \rightarrow \pm 1$, we respectively get the symmetric triplet subspace \mathbb{G}_+ and antisymmetric singlet subspace \mathbb{G}_- :

$$\mathbb{G}_+ = \left\{ |00\rangle, |11\rangle, \frac{|01\rangle + |10\rangle}{\sqrt{2}} \right\} \text{ and } \mathbb{G}_- = \left\{ \frac{|01\rangle - |10\rangle}{\sqrt{2}} \right\}. \quad (1.3)$$

Higher-dimensional multiparticle Hilbert spaces are constructed in the similar fashion, requiring that the associated ket states are even or odd under any two-particle exchange, in the case of bosonic or fermionic statistics, respectively. These are the only two allowed options for fundamental particles in the *Standard Model*: **matter** particles being all fermions while **force** particles being all bosons.

1.2 (Classical) topology

According to *Wikipedia*: “In mathematics, *topology* (from the Greek words for ‘place, location’ and ‘study’) is concerned with the properties of a geometric object that are preserved under continuous deformations, such as stretching, twisting, crumpling, and bending; that is, without closing holes, opening holes, tearing, gluing, or passing through itself.”

Perhaps the most graphic illustration of topology is provided by the *knot theory*. A knot is an embedding of a circle in three-dimensional Euclidean space. Two knots are equivalent if they can be smoothly transformed one into the other, without cutting the knotted string. Two knots can be added by locally cutting and joining them as sketched in the illustration. This does depend on choosing their relative orientation, yielding two possible outcomes. Endowing knots with a fixed orientation and joining them consistently, this twofold ambiguity would be suppressed. The knot sum of oriented knots is *commutative* and *associative*.

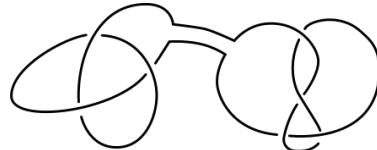


Figure 1.2: Adding two knots.

A knot is *prime* if it is nontrivial and cannot be decomposed into a sum of two nontrivial knots. Otherwise it is called *composite*. This leads to the notion of the *prime decomposition*, which is unique for the oriented knots. Below, we show all the prime knots, up to seven crossings. 3_1 is the simplest nontrivial knot known as the *trefoil knot*. Amusingly, a knot in three dimensions can be untied when placed in a four-dimensional space. It is also true that one cannot form the *unknot* in three dimensions by adding two nontrivial knots.

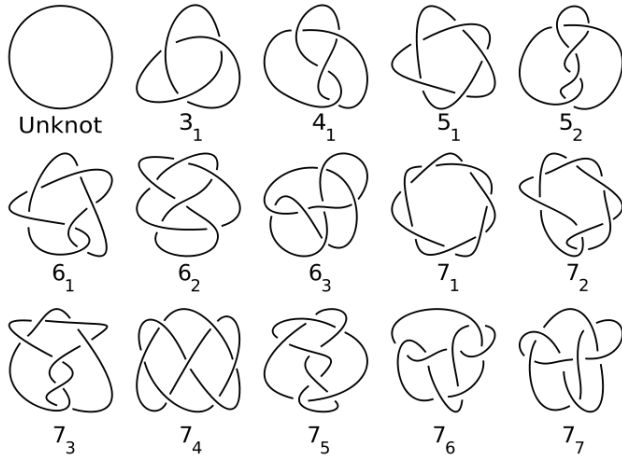


Figure 1.3: A chart of all prime knots with seven or fewer crossings, not including mirror images, plus the trivial unknot (which is not considered prime).

1.3 The braid group

Another elementary example of algebraic constructions rooted in topology is the *braid group*. This topic is closely related to the knot theory but is in fact only a step away from the *topological quantum computing*. The braid group on n strands B_n consists of n -braids whose group operation is composition of braids. A braid is produced by starting with n distinct points on a plane and evolving them along the third (say time) axis to end up at the same, albeit reshuffled, positions, while never crossing each other. The equivalence of braids is understood analogously to the equivalence of knots. A couple examples of braid composition, reading evolution from left to right, are shown below.

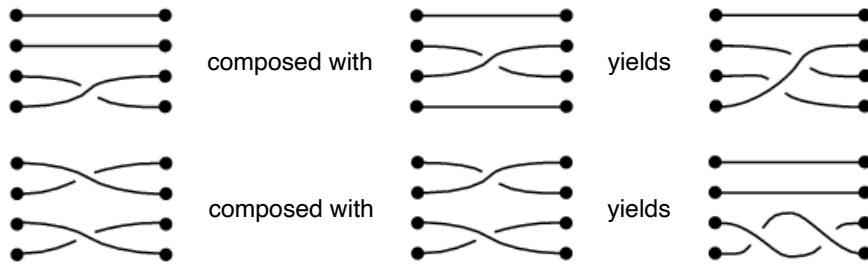


Figure 1.4: Composition of braids.

The entire braid group B_n can in fact be produced using $n - 1$ generators: $\sigma_1, \sigma_2, \sigma_3, \dots, \sigma_{n-1}$, which are shown below for the above example of $n = 4$. The generators satisfy the following fundamental properties (noting that the group is *non-Abelian*):

$$\sigma_i \sigma_j = \sigma_j \sigma_i, \quad |i - j| \geq 2 \quad (1.4)$$

and

$$\sigma_i \sigma_{i+1} \sigma_i = \sigma_{i+1} \sigma_i \sigma_{i+1}, \quad i = 1, 2, \dots, n - 2, \quad (1.5)$$

which is known as the *Yang-Baxter relation*. These identities suffice for demonstrating the equivalence of two braids decomposed into their generators.

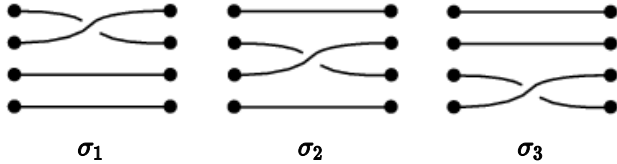


Figure 1.5: Elementary braid generators of B_4 .

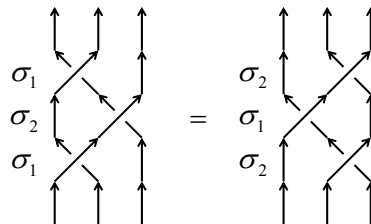


Figure 1.6: Yang-Baxter relation (1.5) between two braids, which correspond to twisting two side threads (*worldlines*) around the central one, which stays fixed.

1.4 Quantum statistics of anyons

We are now ready to formulate the concept of *anyonic* quantum statistics in *two* spatial dimensions. It will generalize the notion of bosonic/fermionic statistics of fundamental particles. Let us proceed axiomatically and then provide some concrete physical examples. I will mainly follow Ref. [5]. A nice quick rundown is also given in Ref. [7], while a more in-depth account can be found in Ref. [6].

1.4.1 Fusion spaces

Imagine we have several types of particles (called *anyons*) labelled by a, b, \dots , which constitute the list

$$M = \{1, a, b, \dots\}. \quad (1.6)$$

1 was added to correspond to the *vacuum* (i.e., the physical many-body ground state) devoid of any anyons. $c \in M$ is a *topological charge* that cannot be changed by any *local* perturbation, so long as the associated anyon is well separated from all other particles.

Combining two anyons, a and b (by bringing them together and letting them interact), follows the physical structure according to the *fusion rules* (which are Abelian and associative):

$$a \times b = \sum_{c \in M} N_{ab}^c c. \quad (1.7)$$

We require that $1 \times a = a$, $\forall a$. *Fusion coefficients* $N_{ab}^c = 0, 1, 2, \dots$ are natural numbers, which describe *topological charges (fusion channels)* a composite of a and b can carry. The possible values are in M , for all c such that $N_{ab}^c = 1$. $N_{ab}^c = 2$ or higher (which are uncommon) would signify multiple distinct quantum states you can fuse into, producing the same topological charge c . You are allowed to form quantum superpositions only of anyon configurations that fuse to give the same topological charge. We can also think in reverse and see how a topological charge can splinter into possible sets of anyons. The allowed anyonic outcomes of fusion should not depend on the exact sequence of fusions, which constrains the structure of the fusion rules.

We will, furthermore, require that there is a conjugation operator C , which maps any $a \in M$ as

$$C : a \mapsto \bar{a} \mapsto a, \quad (1.8)$$

such that fusing $a \times \bar{a}$ may yield vacuum 1. \bar{a} is called the *antiparticle* of a , which we need in order to be able to initialize a multi-anyon state out of vacuum. Some particles may be self-conjugate, i.e., $\bar{a} = a$, which is also true for the vacuum: $\bar{1} = 1$.

For a set of anyons a, b, c, \dots that are placed at some classical positions $1, 2, 3, \dots$, say stringed along some axis in 1D, from left to right, we may have a nontrivial degeneracy of the corresponding lowest-energy manifold (in which case, the anyons are called *nonabelions*). The degeneracy is established by progressively adding all N_{ab}^c 's for each allowed pairwise fusion and cascading down the fusion graph until we end up with a single particle, which defines the net topological charge. The orthonormal basis states of the original multi-anyon configuration can be labelled according to the resultant fusion outcomes, with different choices for the exact pairwise fusion sequence resulting in a unitary transformation matrix F .

Example: Fibonacci anyons.— Mathematically simplest example of non-Abelian anyons is provided by *Fibonacci anyons*. This model is based on a single nontrivial anyon τ (which is thus its own antiparticle: $\bar{\tau} = \tau$) that satisfies the fusion rule

$$\tau \times \tau = 1 + \tau. \quad (1.9)$$

Any system thus may have the total topological charge of 1 or τ , with the corresponding dimensionality growing in peculiar way, as a function of the anyon number. For 3, 4, and 5 anyons,

$$\begin{aligned} \tau \times \tau \times \tau &= 1 + 2\tau, \\ \tau \times \tau \times \tau \times \tau &= 2 + 3\tau, \\ \tau \times \tau \times \tau \times \tau \times \tau &= 3 + 5\tau, \end{aligned} \quad (1.10)$$

etc., such that the dimensionality corresponding to N anyons with total topological charge of 1 (τ) is given by the Fibonacci sequence starting with 1, 1, \dots (1, 2, \dots), hence the name.

A qbit requires at least three anyons, to be able to form a two-dimensional subspace with the same topological charge. These are given by

$$|0\rangle = |((\bullet, \bullet)_0, \bullet)_1\rangle \quad \text{and} \quad |1\rangle = |((\bullet, \bullet)_1, \bullet)_1\rangle, \quad (1.11)$$

→ total topological charge

where the bullets stand for individual anyons and the subscript denotes the fusion outcome: 0 fusing trivially and 1 yielding a Fibonacci anyon. The third, noncomputational state $|NC\rangle = |((\bullet, \bullet)_1, \bullet)_0\rangle$ is discarded. The two computational states thus correspond to either 0 or 1 in the outcome of the fusion of the first pair. Alternatively, a qbit can be formed out of 4 anyons, with the trivial total charge, throwing away three noncomputational states with total charge τ .

$$|0_L\rangle = \text{Diagram } 0_L \quad |1_L\rangle = \text{Diagram } 1_L \quad |NC\rangle = \text{Diagram } NC$$

Figure 1.7: The logic qbit and noncomputational states based on three Fibonacci anyons.

1.4.2 Fusion matrices

The freedom of defining the basis states of the fusion space gives rise to the F (fusion) matrices, which are unitary transformations between bases obtained by following a different pairwise fusion sequence. It is important to be able to relate such different bases in order to later establish the braiding representation in the fusion space. For example, following two different fusion pathways available for three anyons, a , b , and c , ending up with anyon d , defines unitary matrix \hat{F}_{abc}^d , whose elements are labelled according to the charge of the intermediate states, e and f , as shown in the figure (and whose size corresponds to the number of distinct ways for abc to fuse into d along a give graph).

We will assume (as the case in our simple examples) that N_{ab}^c can be only 0 or 1, so we can suppress the additional label that would be needed to account for different fusion states with the same topological charge. The states depicted in the figure below can also be denoted by

$$|(ab)_e, c)_d\rangle = |(a, (bc)_f), d\rangle (\hat{F}_{abc}^d)_e^f, \quad (1.12)$$

summing over the repeated index f . We will always start with a set of anyons, a, b, c, \dots , lined up from left to right in some arbitrary (but fixed) fashion, with the full freedom to rearrange pairwise fusions in such 2D graphs without cutting or crossing any lines.

$$\text{Diagram } a \vee b \vee c \text{ --- } e \text{ --- } d = \text{Diagram } a \vee b \vee c \text{ --- } f \text{ --- } d \sum_f (\hat{F}_{abc}^d)_e^f$$

Figure 1.8: F matrices relating fusion space bases obtained following different fusion diagrams.

1.4.3 Braiding anyons

With the above fusion procedure defining the fusion space within which we define computational states, the actual computation is performed by physically braiding positions of the anyons. The computational gates are thus realized as a unitary *representation* of the braid group B_n , with n being the total number of anyons. We suppose that each pairwise exchange of adjacent anyons, a and b , corresponding to some elementary braid σ_j , engenders a topological phase factor

$$R_{ab}^c = e^{i\theta_{ab}^c}, \quad (1.13)$$

in the fusion state yielding topological charge c . The phase θ_{ab}^c describes the quantum statistical angle $\in [0, 2\pi]$. Doing the same exchange with opposite chirality, corresponding to σ_j^{-1} , yields the opposite phase.

Suppose we work in the three-anyon basis formed by the left-to-right fusion sequence, like $|((ab)_e, c)_d\rangle$ (left graph in Fig. 1.8). In this left basis, the fusion-space representation of the first braid generator, Σ_1 , is given simply by the fundamental phase factor:

$$\Sigma_1|((ba)_e, c)_d\rangle = |((ab)_e, c)_d\rangle e^{i\theta_{ab}^e}. \quad (1.14)$$

Σ_2 , on the other hand, looks simpler in the *right* basis, $|(a, (bc)_f), d\rangle$:

$$\Sigma_2|(a, (cb)_f), d\rangle = |(a, (bc)_f), d\rangle e^{i\theta_{bc}^f}. \quad (1.15)$$

To consistently write them both in the same (say left) basis, we invoke Eq. (1.12):

$$\begin{aligned} \Sigma_2|((ac)_e, b)_d\rangle &= \Sigma_2|(a, (cb)_f), d\rangle (\hat{F}_{acb}^d)_e^f = |(a, (bc)_f), d\rangle e^{i\theta_{bc}^f} (\hat{F}_{acb}^d)_e^f \\ &= |((ab)_g, c)_d\rangle \left[(\hat{F}_{abc}^d)^{-1} \right]_g^f e^{i\theta_{bc}^f} (\hat{F}_{acb}^d)_e^f. \end{aligned} \quad (1.16)$$

In a similar fashion, we can construct all n -braid representations in our fusion space. It turns out the consistency conditions on the F -matrices (known as *pentagon equations*) and braid factors R (*hexagon equations*) are sufficiently severe that one can systematically classify all possible anyonic models up to a given number of distinct topological charges a, b, \dots .

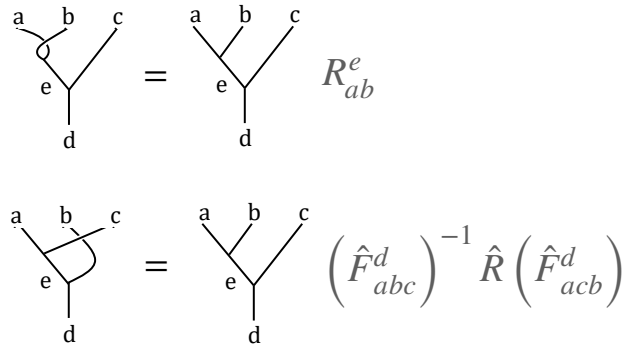


Figure 1.9: Constructing braiding generators for anyons in the *left standard basis*.

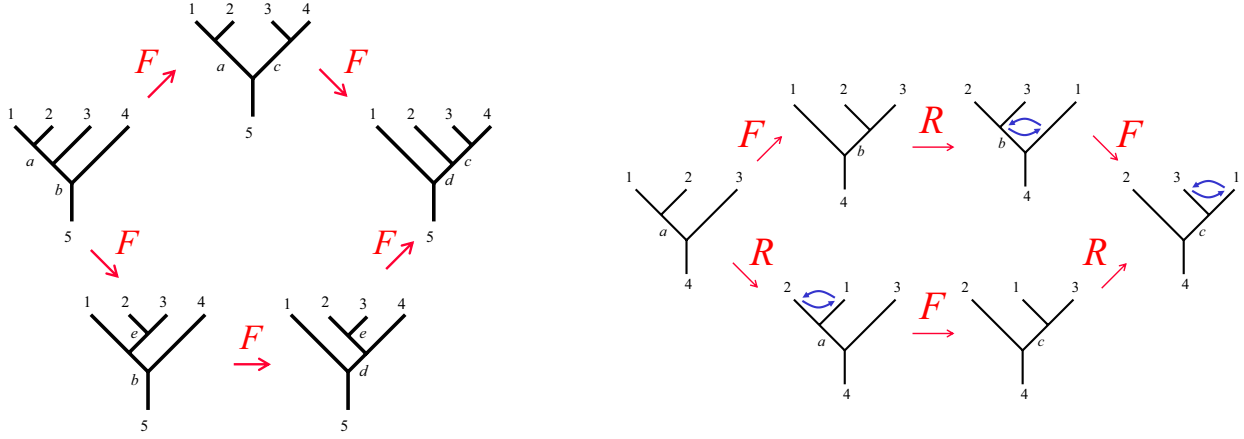


Figure 1.10: Pentagon and hexagon equations [6] that are used to constrain possible forms of F and R . The pentagon equation ensures consistency of the fusion rules, while the hexagon equation guarantees the topological equivalence of different braid sequences. Amusingly, these relations are sufficient to establish an internally consistent anyonic theory.

For Abelian anyons, the fusion space is nondegenerate, so that \hat{F} matrices are absent and the phases engendered by braiding simply add up.

Example: Braiding Fibonacci anyons.— Fibonacci anyon fusion rules (1.10) dictate the following F and R matrices, which are consistent with Fig. 1.10:

$$\hat{F}_{\tau\tau\tau}^{\tau} = \begin{pmatrix} \tau & \sqrt{\tau} \\ \sqrt{\tau} & -\tau \end{pmatrix} \quad \text{and} \quad \hat{R}_{\tau\tau} \equiv \begin{pmatrix} R_{\tau\tau}^1 & 0 \\ 0 & R_{\tau\tau}^{\tau} \end{pmatrix} = \begin{pmatrix} e^{4\pi i/5} & 0 \\ 0 & e^{-3\pi i/5} \end{pmatrix}, \quad (1.17)$$

where $\tau \equiv (\sqrt{5} - 1)/2$ is the inverse of the *golden ratio* $\phi = \tau + 1$. Note that the Fibonacci numbers can be expressed in terms of the golden ratio using *Binet's formula*.

The overarching philosophy here is that the overall result (in terms of the associated unitary evolution) of braiding a sequence of anyons a, b, c, \dots into some rearrangement thereof, e.g., c, a, b, \dots , should not depend on the exact sequence of braids, for a given element of the braid group B_n . In other words, the result should only depend on the topological *equivalence classes* that make up B_n , thus realizing a unitary *representation* of B_n in the fusion space, if the sequence a, b, c, \dots maps back onto itself. In particular, braiding in reverse realizes the inverse transformation.

Chapter 2

Quantum computing with anyons

2.1 Executing topological QC

1. *Initialization:* m particle-antiparticle pairs, $c_1\bar{c}_1, c_2\bar{c}_2 \dots, c_m\bar{c}_m$ are created locally out of vacuum, with each pair thus having a trivial total charge.
2. *Processing:* The $2m$ particles are adiabatically braided along some predetermined worldlines.
3. *Readout:* Neighboring pairs are fused together, recording whether each pair annihilates fully or not. This record is the output of the computation.

In the computational (logic) basis of the Fibonacci anyons, shown in Fig. 1.7, the readout would boil down to fusing only the first pair of each anyonic triplet. As long as our braiding is designed to never populate the noncomputational states, there is no need to fuse the third anyon (apart from the consistency check, which should always yield 1).

2.2 Computing with Ising anyons

A model that is slightly more complex but experimentally more promising is given by the Ising anyons. Despite being more complex, this model does not realize universal quantum computing in its pristine (topologically protected) form, in contrast to the Fibonacci anyons. There are two particles here - Ising anyons σ and ordinary fermions ψ , which follow fusion rules:

$$\begin{aligned}\sigma \times \sigma &= 1 + \psi, \\ \sigma \times \psi &= \sigma, \\ \psi \times \psi &= 1.\end{aligned}\tag{2.1}$$

Both types of particles are thus their own antiparticles. Carrying out repeated application of the fusion rules to a string of Ising anyons,

$$\begin{aligned}\sigma \times \sigma \times \sigma &= 2\sigma, \\ \sigma \times \sigma \times \sigma \times \sigma &= 2 + 2\psi, \\ \sigma \times \sigma \times \sigma \times \sigma \times \sigma &= 4\sigma,\end{aligned}\tag{2.2}$$

we see that we need at least three anyons to realize a single qbit (with net topological charge σ) or four anyons fusing to 1. These fusion rules dictate the following F/R matrix structure for the Ising anyons:

$$\hat{F}_{\sigma\sigma\sigma}^{\sigma} = \frac{1}{\sqrt{2}} \begin{pmatrix} 1 & 1 \\ 1 & -1 \end{pmatrix} \quad \text{and} \quad \hat{R}_{\sigma\sigma} \equiv \begin{pmatrix} R_{\sigma\sigma}^1 & 0 \\ 0 & R_{\sigma\sigma}^{\psi} \end{pmatrix} = e^{-i\pi/8} \begin{pmatrix} 1 & 0 \\ 0 & e^{i\pi/2} \end{pmatrix}. \tag{2.3}$$

Two-qbit computational basis based on 6 anyons is shown in the figure. Starting in the vacuum state and following the graph in reverse, we can initialize the $|00\rangle$ state by creating three conjugate pairs of σ, σ out of vacuum 1.

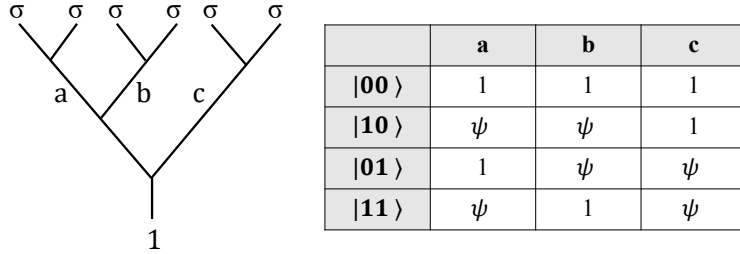


Figure 2.1: The fusion diagram for six Ising anyons for a pairwise basis restricted to the global vacuum sector.

A realistic and engineerable physical system that displays such anyonic statistics is provided by a network of delicately tuned *superconducting wires*. In the underlying model, we can explicitly see how a fermionic electron *fractionalizes* into two Ising anyons, $\psi \rightarrow \sigma \times \sigma$, engendered by *Majorana* fermions. Two fermions, in turn, fuse to form a *Cooper pair*, which can easily dissolve in the superconducting *bosonic condensate* under a local perturbation.

2.3 Majorana zero modes in superconducting wires

Let us start with the *second-quantized* Hamiltonian for a *spinless* (effectively spin-polarized, in practice) 1D superconductor [4]:

$$H = \sum_{m=1}^{N-1} \left[\left(-w c_{m+1}^\dagger c_m + \Delta c_{m+1}^\dagger c_m^\dagger \right) + \text{H.c.} \right] - \mu \sum_{m=1}^N \left(c_m^\dagger c_m - \frac{1}{2} \right). \tag{2.4}$$

The *hopping* w and *pairing gap* Δ can be chosen (in a convenient *gauge*) to be real and non-negative. The *chemical potential* μ is necessarily real. c_m/c_m^\dagger are fermionic *creation/annihilation* operators along a chain of N sites, obeying standard anticommutation algebra:

$$\{c_m, c_n^\dagger\} = \delta_{mn}, \quad \{c_m, c_n\} = \{c_m^\dagger, c_n^\dagger\} = \delta_{mn}. \quad (2.5)$$

Next, we switch to the *Majorana representation* of the fermionic statistics. Namely, for each fermion labelled by m , we define two *Majorana fermions*, γ_m and γ'_m , s.t.

$$c_m = \frac{\gamma_m + i\gamma'_m}{2}, \quad (2.6)$$

where (one can think of γ_m as standing for the “real” and γ'_m “imaginary” parts of c_m)

$$\gamma_m \equiv c_m + c_m^\dagger \quad \text{and} \quad \gamma'_m \equiv \frac{c_m - c_m^\dagger}{i} \quad (2.7)$$

are self-adjoint operators obeying the anticommutation relations

$$\{\gamma_k, \gamma_l\} = 2\delta_{kl}, \quad (2.8)$$

where k and l label both the site and the Majorana type (i.e., primed or unprimed). The fermion number operator then decomposes as

$$n_m \equiv c_m^\dagger c_m = \frac{i\gamma_m \gamma'_m + 1}{2}. \quad (2.9)$$

The Hamiltonian (2.4) now becomes, in this notation,

$$H = -\frac{iw}{2} \sum_{m=1}^{N-1} (\gamma_m \gamma'_{m+1} - \gamma'_m \gamma_{m+1}) + \frac{i\Delta}{2} \sum_{m=1}^{N-1} (\gamma_m \gamma'_{m+1} + \gamma'_m \gamma_{m+1}) - \frac{i\mu}{2} \sum_{m=1}^N \gamma_m \gamma'_m. \quad (2.10)$$

In the special case when $\Delta = w$ and writing $\mu \equiv -2v$, this simplifies to

$$H = iv \sum_{m=1}^N \gamma_m \gamma'_m + iw \sum_{m=1}^{N-1} \gamma'_m \gamma_{m+1}. \quad (2.11)$$

The two extreme cases of $w = 0$, $v \neq 0$ and $w \neq 0$, $v = 0$ are depicted in the figure, where the lower, A sublattice stands for the unprimed Majoranas and the upper, B sublattice for the primed Majoranas. Each dimer in the upper panel corresponds to the Majorana decomposition of a single (m th) electron. This discussion parallels the *SSH model* for the electronic band structure in the organic polymer polyacetylene ($C_2H_2)_N$ [2].

The v term should be thought of as tending to restore the original fermion (2.6) on the same physical site m , while the w term strives to form a new fermion by fusing Majoranas from the adjacent sites:

$$c'_m = \frac{\gamma'_m + i\gamma_{m+1}}{2}. \quad (2.12)$$

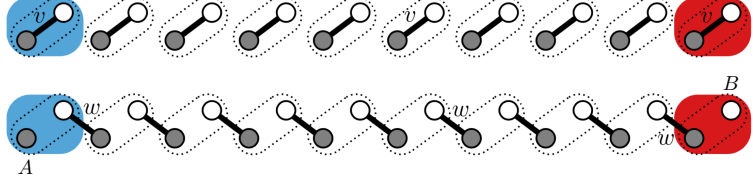


Figure 2.2: Fully-dimerized limits: $w = 0$ (top) or $v = 0$ (bottom) corresponding respectively to the nontopological chain of isolated fermions and a *topological superconductor*.

The corresponding Hamiltonians are then (dropping unimportant constants)

$$H \rightarrow \frac{v}{2} \sum_{m=1}^N c_m^\dagger c_m \quad \text{and} \quad H \rightarrow \frac{w}{2} \sum_{m=1}^{N-1} c_m^\dagger c'_m, \quad (2.13)$$

according to the respective particle-number operators.

Note that in the second case (which is identified as *topologically nontrivial*), the very first, γ_1 , and the very last, γ'_N , Majoranas of the chain dropped out of the Hamiltonian. Together, they define a *fermionic zero mode*

$$c_0 = \frac{\gamma_1 + i\gamma'_N}{2}, \quad (2.14)$$

which is likewise absent from the above second-quantized Hamiltonian (which has $N - 1$ rather than N terms). This means that for any many-body energy eigenstate $|\psi\rangle$ s.t. $c_0|\psi\rangle = 0$, $c_0^\dagger|\psi\rangle$ is another eigenstate with exactly the same energy. If v is finite but $|v| < w$, the zero mode acquires a finite energy, which is exponentially small, $\sim e^{-N/\xi}$, in system size N , with a correlation length ξ that diverges when $|v| \rightarrow w$.

Crucially, a domain wall between two topologically distinct regions (one trivial the other nontrivial) necessarily hosts a single unpaired Majorana fermion, as sketched in the figure below. These Majoranas, which are bound to potentially mobile domain walls can now be used for braiding in a superconducting wire networks. This was thoroughly discussed in Ref. [1], where the motion of domain walls can, for example, be realized by using tunable electrostatic gates applied to the wires. A basic T -junction for realizing a Majorana exchange is sketched below. The fusion is realized simply by bringing two Majoranas together and letting them hybridize into either vacuum 1 or fermionic ψ state (which has measurable signatures, for example, either electrostatically or spectrally).

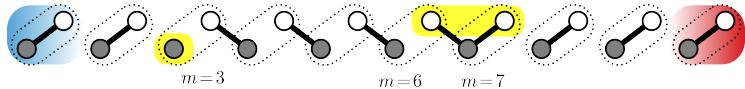


Figure 2.3: A pair of domain walls in the dimerized regime, hosting two zero-energy Majoranas: in cell 3 (sublattice A) and shared by cells 6 and 7 (sublattice B) within a *trimer*.

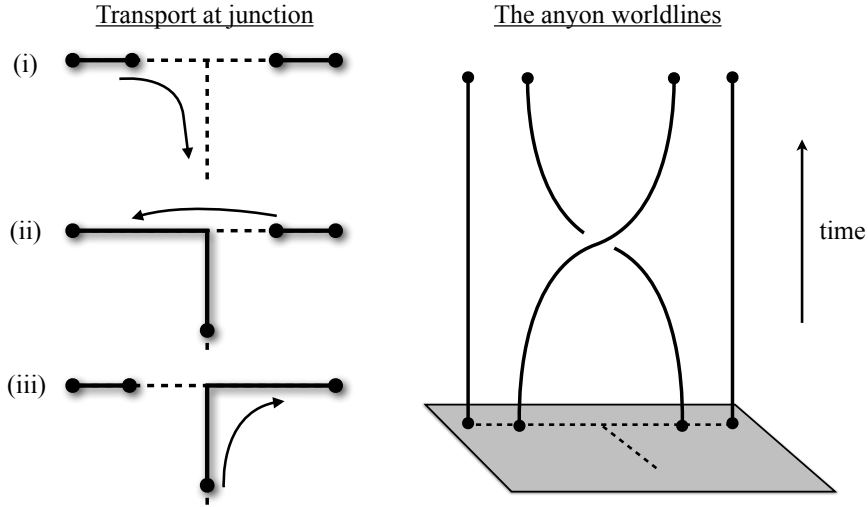


Figure 2.4: A T -junction provides the simplest wire network that enables meaningful adiabatic exchange of Majorana fermions.

2.4 Universal computing with Fibonacci anyons

While the Majorana fermions appear experimentally attractive, they do come with one serious deficiency: They cannot realize, in their pure form, a universal quantum computer. Amusingly, this can, however, be accomplished with the formally simpler Fibonacci anyons. Their own catch is that the experimental prospects seem much bleaker. Nevertheless, we summarize below the key ideas that go into realizing a scalable universal quantum computer based on the logic basis shown in Fig. 1.7.

Braid Topologies for Quantum Computation

N. E. Bonesteel, L. Hormozi, and G. Zikos

Department of Physics and National High Magnetic Field Laboratory, Florida State University, Tallahassee, Florida 32310, USA

S. H. Simon

Bell Laboratories, Lucent Technologies, Murray Hill, New Jersey 07974, USA

(Received 23 May 2005; published 29 September 2005)

In topological quantum computation, quantum information is stored in states which are intrinsically protected from decoherence, and quantum gates are carried out by dragging particlelike excitations (quasiparticles) around one another in two space dimensions. The resulting quasiparticle trajectories define world lines in three-dimensional space-time, and the corresponding quantum gates depend only on the topology of the braids formed by these world lines. We show how to find braids that yield a universal set of quantum gates for qubits encoded using a specific kind of quasiparticle which is particularly promising for experimental realization.

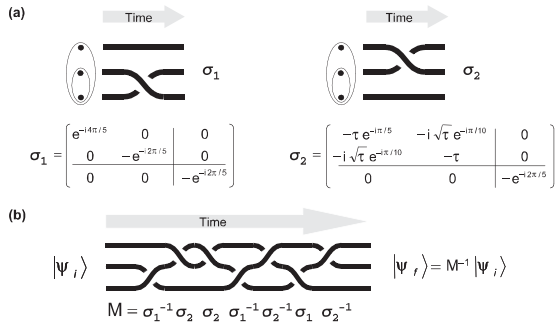


FIG. 2. (a) Elementary three-quasiparticle braids. The pictures represent quasiparticle world lines in $2 + 1$ -dimensional space-time, with time flowing from left to right. The matrices σ_1 and σ_2 are the transition matrices produced by these elementary braids which act on the three-dimensional Hilbert space shown in Fig. 1. Here $\tau = (\sqrt{5} - 1)/2$ is the inverse of the golden mean. The upper 2×2 blocks of these matrices act on the computational qubit space (total q -spin 1) and are used to perform single-qubit rotations, while the lower right element is a phase which multiplies $|NC\rangle$. (b) A general three-quasiparticle braid and the corresponding matrix expression for the transition matrix it produces. Here $|\Psi_i\rangle$ is the initial state and $|\Psi_f\rangle$ the final state after braiding. Note that these (and subsequent) figures only represent the topology of the braid. In any actual implementation, quasiparticles will have to be kept sufficiently far apart to keep from lifting the topological degeneracy.

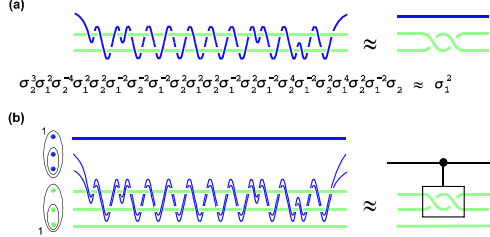


FIG. 3 (color online). (a) A three-quasiparticle braid in which one quasiparticle is woven around two static quasiparticles and returns to its original position (left), and yields approximately the same transition matrix as braiding the two stationary quasiparticles around each other twice (right). The corresponding matrix equation is also shown. To characterize the accuracy of this approximation, we define the distance between two matrices, U and V , to be $\epsilon = \|U - V\|$, where $\|O\|$ is the operator norm of O equal to the square-root of the highest eigenvalue of $O^\dagger O$. The distance between the matrices resulting from the actual braiding (left) and the desired effective braiding (right) is $\epsilon \approx 2.3 \times 10^{-3}$. (b) A two-qubit braid constructed by weaving a pair of quasiparticles from the control qubit (top) through the target qubit (bottom) using the weaving pattern from (a). The result of this operation is to effectively braid the upper two quasiparticles of the target qubit around each other twice if the control qubit is in the state $|1_L\rangle$, and otherwise do nothing. This is an entangling two-qubit gate which can be used for universal quantum computation. Since all effective braiding takes place within the target qubit, any leakage error is due to the approximate nature of the weave shown in (a). By systematically improving this weave using the Solovay-Kitaev construction, leakage error can be reduced to whatever level is required for a given computation.

Figure 2.5: Summary of Ref. [3], which showed how to realize universal quantum computing based on intricate weaving of Fibonacci anyons.

Bibliography

- [1] J. Alicea, Y. Oreg, G. Refael, F. von Oppen, and M. P. A. Fisher. Non-abelian statistics and topological quantum information processing in 1d wire networks. *Nat. Phys.*, 7:412–417, 2011.
- [2] J. K. Asbóth, L. Oroszlány, and A. Pályi. *A Short Course on Topological Insulators*. Springer, Heidelberg, 2016.
- [3] N. E. Bonesteel, L. Hormozi, G. Zikos, and S. H. Simon. Braid topologies for quantum computation. *Phys. Rev. Lett.*, 95:140503, Sep 2005.
- [4] A. Kitaev and C. Laumann. Topological phases and quantum computation. In *Exact Methods in Low-dimensional Statistical Physics and Quantum Computing*, pages 101–125. Oxford University Press, Oxford, 2010. arXiv:0904.2771.
- [5] V. T. Lahtinen and J. K. Pachos. A short introduction to topological quantum computation. *SciPost Phys.*, 3:021, 2017.
- [6] J. Preskill. Lecture notes for physics 219: Quantum computation. Lecture Notes, 2004.
- [7] M. K. Spillane. An introduction to the theory of topological quantum computing. 2008.